Screening Lengths in Ionic Fluids

Fabian Coupette,[1] Alpha A. Lee,[2] and Andreas Härtel[1,*]
[1]Institute of Physics, University of Freiburg, Hermann-Herder-Straße 3, 79104 Freiburg, Germany
[2]Cavendish Laboratory, JJ Thomson Avenue, Cambridge CB3 0HE, United Kingdom

(Received 28 March 2018; published 14 August 2018)

The decay of correlations in ionic fluids is a classical problem in soft matter physics that underpins applications ranging from controlling colloidal self-assembly to batteries and supercapacitors. The conventional wisdom, based on analyzing a solvent-free electrolyte model, suggests that all correlation functions between species decay with a common decay length in the asymptotic far field limit. Nonetheless, a solvent is present in many electrolyte systems. We show using an analytical theory and molecular dynamics simulations that multiple decay lengths can coexist in the asymptotic limit as well as at intermediate distances once a hard sphere solvent is considered. Our analysis provides an explanation for the recently observed discontinuous change in the structural force across a thin film of ionic liquid-solvent mixtures as the composition is varied, as well as reframes recent debates in the literature about the screening length in concentrated electrolytes.

DOI: 10.1103/PhysRevLett.121.075501

The study of ionic fluids and electrolytes has received significant interest in recent times due to its central relevance to a plethora of technological applications, ranging from controlling colloidal self-assembly [1] to supercapacitors and batteries [2]. The challenge deals with the rich physics that arise from competing long-ranged Coulomb interactions and the steric repulsion of particles. The arrangement of ions in bulk and near interfaces governs properties such as capacitance [3–5] and effective forces between colloids [6]; thus a physics understanding of how ion-ion correlations decay and how electric fields are screened is central to designing fit for purpose electrolytes.

The decay of correlations in ionic fluids is a classical problem in soft matter and liquid state physics [7,8]. According to the conventional wisdom, all correlation functions in a simple fluid mixture where particles interact via short-ranged and Coulomb interactions decay asymptotically in the same form, i.e., $e^{-r/\lambda}\cos(\omega r-\tau)/r$, and, crucially, the decay length λ—synonymously the screening length—and oscillation frequency ω are the same for all correlation functions [9]. This common decay has been explicitly verified for the restricted primitive model (RPM), a simple binary solvent-free electrolyte model that is paradigmatic in electrolyte physics—it has been shown that the cation-cation, cation-anion, and anion-anion correlation functions all decay with the same decay length and oscillation frequency [10,11], which has also been used for the interpretation of experiments [12–14]. However, in technological applications, ions are usually mixed with a solvent in order to enhance conductivity and reduce viscosity [15–17]. This raises the important question of how the presence of solvents influences ion-ion correlations.

Recent surface force balance experiments show that the disjoining force between charged surfaces across ionic liquid-solvent mixtures decays in an oscillatory manner with an exponentially decaying envelope [14,18,19]. However, as the ion concentration is increased, the oscillation frequency undergoes a steplike transition [14]—at low ion concentration, it is comparable to the size of the solvent molecule, whereas for concentrated electrolytes it is comparable to the size of an ion pair. This is qualitatively reminiscent of structural crossover in a binary mixture of "big" and "small" colloids [20–22]. However, an ion-solvent mixture is evidently at least a three component system and a corresponding mechanism in electrolyte-solvent mixtures is, perhaps surprisingly, hitherto unknown.

In this Letter, we demonstrate that the decay of correlation functions in a simple fluid mixture is not necessarily unique; i.e., there is no common asymptotic decay length and oscillation wavelength. By considering a hard sphere electrolyte in a hard sphere solvent—one of the simplest possible extensions of the paradigmatic RPM model that includes the physics of electrolyte-solvent interactions—we show theoretically that ion-ion correlations and ion-solvent correlations can have different asymptotic decay lengths and support this result using simulations. These decays are either density- or charge-driven and related to the length scales of steric and Coulombic interactions. While ion-solvent correlations are not affected by charge correlations, ion-ion correlations decay according to a superposition of both effects. However, asymptotic decay is determined by the slowest decaying contribution, which strongly varies with the system composition. Our theory explains the experimentally observed switch of the structural force as the crossover from density-driven to

charge-driven decay [14]. Moreover, it illustrates the importance of space-filling solvent, an often overlooked piece of physics in the theoretical modeling of electrolytes.

To concretize ideas, we consider a hard sphere ion-solvent mixture (HISM) [23–26] throughout this Letter: the ions and solvent are modeled as hard spheres of the same diameter d. The ions (solvent) with number density ρ (ρ_0) carry point charges $Z_\pm = \pm e$ ($Z_0 = 0$). The dielectric nature of the solvent is modeled by a homogeneous dielectric background with a relative permittivity ε. The pair interaction potential between two particles of species ν, $\nu' \in \{+, -, 0\}$ at separation r is given by

$$v_{\nu\nu'}(r) = \begin{cases} \infty & r < d \\ k_B T \lambda_B \frac{Z_\nu Z_{\nu'}}{r} & r \geq d, \end{cases} \tag{1}$$

where $\lambda_B = e^2/(4\pi\epsilon_0 \epsilon k_B T)$ denotes the Bjerrum length and k_B Boltzmann's constant.

Figure 1 shows that the HISM model can have two distinguished coexisting screening lengths at a finite range. We performed MD simulations of the HISM in an equilibrated bulk system using the ESPResSo package [27,28]. Hard particle interactions are modeled using a shifted and truncated purely repulsive Lennard-Jones potential $4\epsilon[(\sigma/r)^{12} - (\sigma/r)^6 + c_{\text{shift}}]$ with $\epsilon = 10^4 k_B T$ and $\sigma = 2^{-1/6} d$. The simulations are performed in a cubic box of volume $V = L \times L \times L$ with periodic boundaries and $L = 30d$. We used $d = 0.3$ nm and $\lambda_B = 0.7$ nm, which corresponds to $\varepsilon \approx 80$ and $T \approx 300$ K. At ionic concentration $\rho = 1$ M and solvent concentration $\rho_0 = 10$ M, Fig. 1(a) clearly shows two coexisting decay lengths with oscillatory and purely exponential decay, respectively, at intermediate separations. Figure 1(b) shows that at a higher solvent concentration $\rho_0 = 40$ M, both ion-ion and ion-solvent correlations share the same intermediate decay length and oscillation wavelength. Our theory (see below) predicts that this finite range decay is the same as the asymptotic decay.

To explain the origin of those coexisting decay lengths, we turn to a theoretical description of HISM based on the density functional theory (DFT) formalism [29]. Within DFT, the free energy is expressed as a functional of one-body densities [29]. For HISM, we can split the pair potential into hard core and electrostatic contributions, $v_{\nu\nu'} = v^{\text{hs}}_{\nu\nu'} + v^{\text{es}}_{\nu\nu'}$. The difference between ideal gas free energy and the exact free energy can be partitioned into three components [29],

$$F = F^{\text{hs}} + F^{\text{es}} + F^{\text{corr}}, \tag{2}$$

where F^{hs} is the hard sphere contribution, F^{es} the electrostatic contribution, and F^{corr} a correlation term that contains remaining contributions. The splitting in Eq. (2), although mathematically trivial, allows us to identify symmetries in the corresponding direct correlations $c^{\text{hs}}_{\nu\nu'}$, $c^{\text{es}}_{\nu\nu'}$, and $c^{\text{corr}}_{\nu\nu'}$. The latter follow from a second functional derivative of the excess free energy with respect to the density, i.e.,

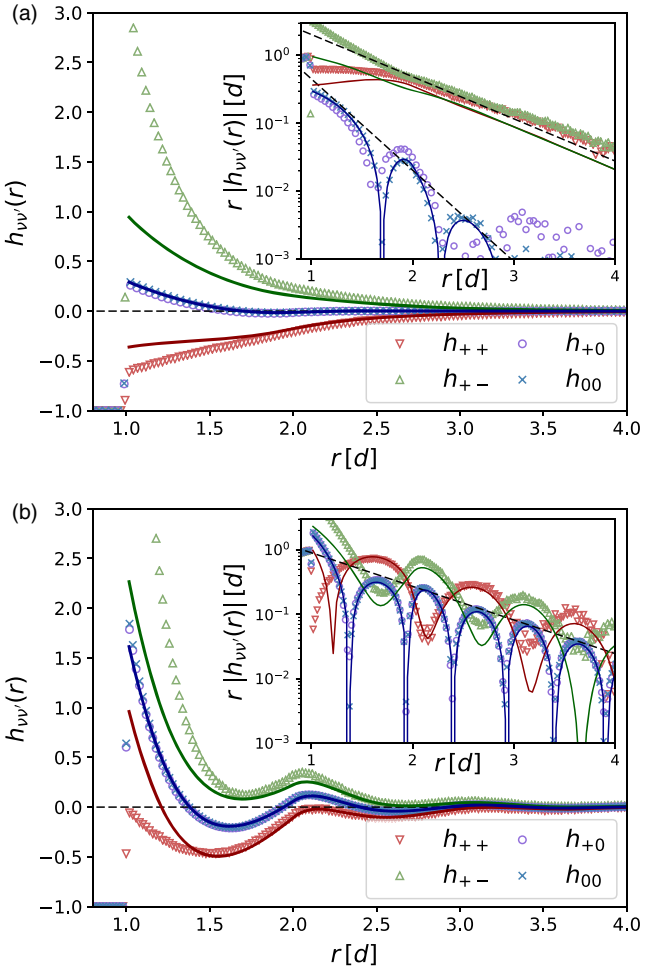

FIG. 1. Total pair-correlation functions $h_{\nu\nu'}(r)$ for ion concentration $\rho = 1$ M and concentration of neutral particles (a) $\rho_0 = 10$ M and (b) $\rho_0 = 40$ M. Symbols represent data from MD simulations and lines from our theory. For symmetry reasons, we only show data for the four given combinations of species. The insets show the same data but plotted on a semilogarithmic scale. Dashed lines represent the predicted monotonic decay $\exp(-r/\lambda_{\nu\nu'})$ with screening length $\lambda_{\nu\nu'}$ from theory.

$$c_{\nu\nu'}(r) = -\frac{1}{k_B T} \frac{\delta^2 F}{\delta\rho_\nu(\mathbf{r}_1)\delta\rho_{\nu'}(\mathbf{r}_2)}, \tag{3}$$

where the homogeneity of the bulk implies $r = |\mathbf{r}_1 - \mathbf{r}_2|$. The hard sphere contribution depends only on the macroscopic packing fraction and the particle diameter d, and therefore, it scales equally with the number density of each component. From F^{es} given by [29]

$$F^{\text{es}} = \frac{1}{2} \sum_\nu \sum_{\nu'} \int \int \rho_\nu(\mathbf{r}) \rho_{\nu'}(\mathbf{r}') v^{\text{es}}_{\nu\nu'}(\mathbf{r}, \mathbf{r}') d\mathbf{r}\, d\mathbf{r}' \tag{4}$$

the electrostatic contribution follows with

$$c^{\mathrm{es}}_{\nu\nu'}(r) = -\frac{v^{\mathrm{es}}_{\nu\nu'}(r)}{k_B T}. \tag{5}$$

Hence, $c^{\mathrm{es}} \coloneqq c^{\mathrm{es}}_{++} = -c^{\mathrm{es}}_{+-}$. Finally, the correlation term underlies the fundamental symmetries of the system; i.e., positive and negative ions are structurally equivalent such that $c^{\mathrm{corr}}_{++} = c^{\mathrm{corr}}_{--}$, $c^{\mathrm{corr}}_{+-} = c^{\mathrm{corr}}_{-+}$, and $c^{\mathrm{corr}}_{+0} = c^{\mathrm{corr}}_{-0} = c^{\mathrm{corr}}_{0-} = c^{\mathrm{corr}}_{0+}$.

The decomposition in Eq. (2) entails that the most general form of the direct correlation matrix $\mathcal{C}$ in the species basis $\{+,-,0\}$ for the HISM model is given by

$$\mathcal{C} = \begin{pmatrix} c^{\mathrm{hs}} + c^{\mathrm{es}} + c^{\mathrm{corr}}_{++} & c^{\mathrm{hs}} - c^{\mathrm{es}} + c^{\mathrm{corr}}_{+-} & c^{\mathrm{hs}} + c^{\mathrm{corr}}_{+0} \\ c^{\mathrm{hs}} - c^{\mathrm{es}} + c^{\mathrm{corr}}_{+-} & c^{\mathrm{hs}} + c^{\mathrm{es}} + c^{\mathrm{corr}}_{++} & c^{\mathrm{hs}} + c^{\mathrm{corr}}_{+0} \\ c^{\mathrm{hs}} + c^{\mathrm{corr}}_{+0} & c^{\mathrm{hs}} + c^{\mathrm{corr}}_{+0} & c^{\mathrm{hs}} + c^{\mathrm{corr}}_{00} \end{pmatrix}. \tag{6}$$

To proceed, we need to relate the direct correlation functions to the total correlation functions $h_{\nu\nu'} = (\mathcal{H})_{\nu\nu'}$, the observables in simulations and experiments. We use the Ornstein-Zernike relation in Fourier space

$$\hat{\mathcal{H}} = (\mathbb{1} - \hat{\mathcal{C}}\varrho)^{-1}\hat{\mathcal{C}}, \tag{7}$$

where we introduced a number density matrix $\varrho = \mathrm{diag}(\rho, \rho, \rho_0)$, and $\hat{f}$ denotes the Fourier transformation of a function f. Substituting Eq. (6) into (7) yields an algebraic expression for the total correlation matrix $\hat{\mathcal{H}}$, the eigenvectors of which are given by $\mathbf{w}_{\mathrm{cc}} = (1,-1,0)$, $\mathbf{w}^{+}_{\mathrm{dd}}$, and $\mathbf{w}^{-}_{\mathrm{dd}}$. The former is equal to one of the eigenvectors of the RPM and gives rise to the well established charge-charge correlation $h_{\mathrm{cc}} = h_{++} - h_{+-}$ as an eigenvalue [29]. The eigenvectors $\mathbf{w}^{\pm}_{\mathrm{dd}}$ become stationary in the limit of vanishing $c^{\mathrm{corr}}_{\nu\nu'}$ with (1,1,1) and $(-1,-1,2)$; the first of them gives rise to a density-density correlation, while the second corresponds to an ion-solvent correlation that has a vanishing eigenvalue.

In particular, the resulting total charge-charge correlation function reads

$$\hat{h}_{\mathrm{cc}} = \frac{\hat{c}^{\mathrm{corr}}_{\mathrm{cc}} + 2\hat{c}^{\mathrm{es}}}{1 - \rho(\hat{c}^{\mathrm{corr}}_{\mathrm{cc}} + 2\hat{c}^{\mathrm{es}})}. \tag{8}$$

Transforming it back into real space yields the formal solution

$$\begin{aligned} h_{\mathrm{cc}}(r) &= \frac{1}{2\pi^2 r}\int_0^\infty k\sin(kr)\frac{\hat{c}^{\mathrm{corr}}_{\mathrm{cc}} + 2\hat{c}^{\mathrm{es}}}{1 - \rho(\hat{c}^{\mathrm{corr}}_{\mathrm{cc}} + 2\hat{c}^{\mathrm{es}})}dk \\ &= \frac{1}{2\pi r}\sum_{q\in Q_{\mathrm{cc}}}\Re\left[\mathrm{Res}_q\left(\frac{(\hat{c}^{\mathrm{corr}}_{\mathrm{cc}} + 2\hat{c}^{\mathrm{es}})q\exp(iqr)}{1 - \rho(\hat{c}^{\mathrm{corr}}_{\mathrm{cc}} + 2\hat{c}^{\mathrm{es}})}\right)\right], \end{aligned} \tag{9}$$

where Q_{cc} contains the roots of

$$1 - \rho(\hat{c}^{\mathrm{corr}}_{\mathrm{cc}} + 2\hat{c}^{\mathrm{es}}) = 0 \tag{10}$$

with a positive imaginary part. The second equality in Eq. (9) makes use of the residue theorem and does, therefore, only hold without further analysis if Eq. (10) does not have any purely real solutions and the elements of Q_{cc} are isolated points in the upper complex half plane (we refer to Refs. [9–11,30] for similar derivations). The eigenvalues to $\mathbf{w}^{\pm}_{\mathrm{dd}}$ share a common denominator; i.e., they are a set Q_{dd} of singularities corresponding to the roots with positive imaginary part of the generic equation

$$\begin{aligned} &1 - \rho(2\hat{c}^{\mathrm{hs}} + \hat{c}^{\mathrm{corr}}_{\mathrm{dd}}) \\ &\quad - \rho_0[2\rho(\hat{c}^{\mathrm{corr}}_{+0})^2 + \hat{c}^{\mathrm{corr}}_{00}(1 - \rho\hat{c}^{\mathrm{corr}}_{\mathrm{dd}}) \\ &\quad + \hat{c}^{\mathrm{hs}}(1 - \rho(\hat{c}^{\mathrm{corr}}_{\mathrm{dd}} - 4\hat{c}^{\mathrm{corr}}_{+0} + 2\hat{c}^{\mathrm{corr}}_{00}))] = 0, \end{aligned} \tag{11}$$

where $c^{\mathrm{corr}}_{\mathrm{dd}} \coloneqq c^{\mathrm{corr}}_{++} + c^{\mathrm{corr}}_{+-}$. Note that, Eq. (11) is independent of c^{es}.

The dominant contribution to a total correlation function $h_{\nu\nu'}$ in the asymptotic long-range limit $r \to \infty$ is determined by the (leading) pole $\bar{q}_{\nu\nu'} = \Re[\bar{q}_{\nu\nu'}] + i\Im[\bar{q}_{\nu\nu'}] \in Q_{\nu\nu'}$ with the smallest imaginary part [31]. It is convenient to introduce the decay length $\lambda_{\nu\nu'} = 1/\Im[\bar{q}_{\nu\nu'}]$ and decay oscillation frequency $\omega_{\nu\nu'} = \Re[\bar{q}_{\nu\nu'}]$. This pole causes the asymptotic decay [9,31,32]

$$h_{\nu\nu'}(r \to \infty) \propto \frac{\exp(-r/\lambda_{\nu\nu'})\cos(\omega_{\nu\nu'}r - \tau_{\nu\nu'})}{r}, \tag{12}$$

where $\tau_{\nu\nu'}$ is a phase shift. The pole, however, could be suppressed on intermediate length scales by a small amplitude, such that its contribution would become neglectable. If there are two poles with decay lengths $\lambda_1 > \lambda_2$ but amplitudes $A_1 < A_2$, pole 2 will dominate until $r \gtrsim \log(A_1/A_2)[\lambda_1^{-1} - \lambda_2^{-1}]^{-1}$, which is a long length scale if $A_1 \ll A_2$.

Importantly, two competing decay lengths arise from the solutions to Eqs. (10) and (11). Switching back into the species basis yields the central result of this Letter,

$$\lambda_{++} = \lambda_{+-} = \max[\lambda_{\mathrm{cc}}, \lambda_{\mathrm{dd}}], \tag{13}$$

$$\lambda_{0+} = \lambda_{0-} = \lambda_{00} = \lambda_{\mathrm{dd}}. \tag{14}$$

The charge-charge correlation does not affect solvent correlations, because $\mathbf{w}_{\mathrm{cc}} \perp (0,0,1)$. Notice that we only made use of the fundamental symmetries in HISM. In other words, in general, it is not true that all species correlations decay with the same decay length. Correlations involving solvent particles decay on a length scale λ_{dd} different from the charge-charge correlation length scale λ_{cc}. If $\lambda_{\mathrm{cc}} > \lambda_{\mathrm{dd}}$, two distinct length scales coexist, as we have shown for intermediate ranges in Fig. 1(a). The same applies for the corresponding oscillation frequencies ω_{cc} and ω_{dd}.

Crucially, this implies that while the dominant decay length continuously changes, the oscillation wavelength of ion-ion correlations can rapidly shift.

To illustrate this effect, we proceed by specifying the functional F in our theoretical framework: we use the White Bear mark II functional for the hard-sphere contribution [33] and Eq. (5) with $v^{\mathrm{es}}_{\nu\nu'}(r) = 0$ for $r < d$ for the electrostatic term. By setting $c^{\mathrm{corr}} \equiv 0$, we obtain analytical correlation functions that are sufficient to illustrate the mechanism of the wavelength switch; for the observed systems, deviations due to this approximation mainly occur at particle contact, as shown in Fig. 1.

Figure 2 shows quantitative predictions of our theory for the decay lengths and the oscillation wavelengths in HISM. The density-induced correlation length, λ_{dd}, is a monotonic function of the macroscopic volume fraction because steric correlations are enhanced as the system becomes denser. However, the charge-induced correlation length, λ_{cc}, is a nonmonotonic function of the ion density but independent of the solvent density. Further, this is the length scale of the decay of the effective electrostatic potential that an ion generates. λ_{cc} decreases for an increasing ion density in a dilute electrolyte because ions are surrounded by counterions, and this arrangement progressively screens the electric field that an ion generates. However, past a threshold ion concentration, ion-ion correlations lead to a counterion solvation shell that overcompensates the ionic charge, which causes a second solvation shell to solvate the counterions, triggering an oscillatory decay [7]. In this regime, increasing the ion concentration amplifies ion-ion correlations; thus the screening length grows. The situation, when the charge pole that determines λ_{cc} changes from purely imaginary to complex, i.e., the decay changes from monotonic to oscillatory, is called a Kirkwood transition [34], and here it coincides with the change between decreasing and increasing screening length. When $\lambda_{\mathrm{cc}} > \lambda_{\mathrm{dd}}$, which is the case for a large region of RPM's parameter space, the ion-ion correlations decay with a decay length that is the electrostatic screening length but different from the ion-solvent and solvent-solvent correlations decay (Fig. 2a). For a high solvent concentration, however, we find a regime $\lambda_{\mathrm{dd}} > \lambda_{\mathrm{cc}}$ where all species correlations decay with one common decay length λ_{dd} [see also Fig. 1(b)] but different from the charge-charge decay length. Thus, the electrostatic screening length must be distinguished from the decay length of species correlation functions that is typically observed in experiments.

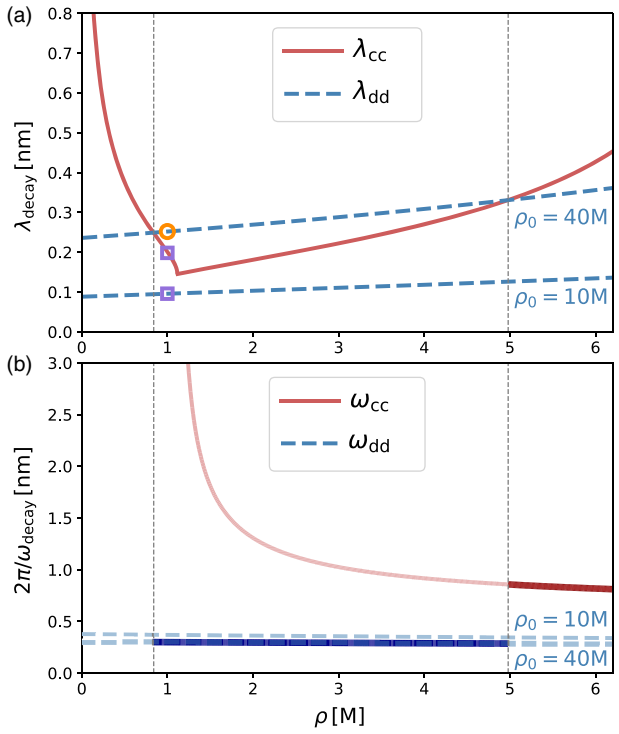

FIG. 2. Theoretical prediction for (a) decay length and (b) inverse oscillation frequency of the leading charge and density pole, respectively, shown against the ion concentration ρ, for $\rho_0 = 10$ M and $\rho_0 = 40$ M with $d = 0.3$ nm and $\lambda_B = 0.7$ nm. Symbols in (a) mark the decay lengths that correspond to the data in Figs. 1(a) (square) and 1(b) (circle). Vertical dashed lines mark points where the asymptotically leading pole changes from charge to density and vice versa for $\rho_0 = 40$ M; leading inverse oscillation frequencies for $\rho_0 = 40$ M are highlighted with bold lines.

Although the ion-ion decay length switches continuously from one pole to another in Figs. 2(a), 2(b) shows that the corresponding oscillation frequency exhibits a discontinuous jump that occurs when the two leading poles have equal imaginary but different real parts. This jump is precisely the effect observed in experimental studies of the surface force across ion-solvent mixtures [14]—the oscillation wavelength switches abruptly. In the experiment, ions and solvent molecules are approximately of the same size, and the oscillation wavelength jumps from d to $2d$, which agrees squarely with the prediction in Fig. 2(b) (see the Supplemental Material [35] for a detailed comparison). Note that, the position of this discontinuous jump in the oscillation wavelength is different from the onset of charge oscillations at the Kirkwood transition, when the real part of the charge pole first takes a finite nonvanishing value [41,42]. Furthermore, the increase of the decay length in Fig. 2(a) accurately describes the decay of the structural force in experiments [14]. However, the experiments show an additional, much longer decay length at large separations, which is neither predicted in our theory, and other recent theoretical studies of underscreening [26,43], nor observed in our simulations on HISM (see Fig. S2 in [35]). This long-ranged decay length might arise from a set of additional poles induced by a mechanism that is not contained in the simplified HISM model. For instance, dipolar solvent-solvent interactions, as present in water, could lead to an additional long decay length. Since this long-ranged decay is experimentally only observed at long distances, the

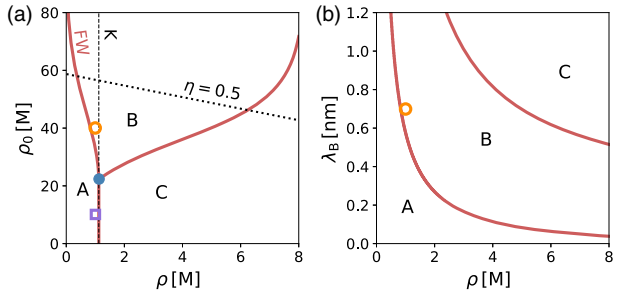

FIG. 3. (a) Different regimes of decay in the ρ—ρ_0 plane of ion and neutral particle concentrations: (A) purely exponential, charge-dominated, (B) oscillatory, exponentially damped, density-dominated, and (C) oscillatory, exponentially damped, charge-dominated. The vertical dashed line represents the Kirkwood line (K) [11,34]. The right boundary of region A represents the Fisher-Widom line (FW) [31,44]. The tilted dashed line marks a total volume fraction $\eta = 0.5$. Symbols are explained in Fig. 2. (b) The same diagram in the ρ—λ_B plane for $\rho_0 = 40$ M.

corresponding leading pole should have a small amplitude and, therefore, could be suppressed at intermediate distances (see Fig. 1).

The three different regimes of asymptotic decay in HISM—purely exponential and charge-dominated decay (A), oscillatory exponentially damped and density-dominated decay (B), and oscillatory exponentially damped and charge-dominated decay (C)—are summarized in Fig. 3. While ion-ion correlations in regions A and C are dominated by the charge pole, ion-ion correlations couple to the solvent in region B. This region appears at high solvent concentrations between A and C, such that the Fisher-Widom line [31,44] of the ions shifts towards lower ion concentrations (away from the Kirkwood line [11,34]). A second branch separates regions A and C, at which the frequency jumps from ω_{dd} to ω_{cc}.

Our conclusions are derived by assuming symmetry between positive and negative ions in Eq. (6). If this symmetry is broken by different ion sizes, all correlation functions couple and share the same set of poles; thus they all decay asymptotically in the same form. However, at intermediate range, simulations of asymmetric ions still exhibit the same coexistence of decay lengths and oscillation frequencies, as shown here for the symmetric case [35]. Consequently, ion size asymmetry can be considered as a perturbation to the symmetric HISM model so that its predictions are still valid for decay lengths in asymmetric systems at (experimentally relevant) intermediate distances.

In summary, we demonstrated the possible coexistence of two asymptotic decay lengths for hard sphere ions in a hard sphere solvent. Our theory explains recent experimental findings concerning a jump of the wavelength of the structural force in ionic fluids [14], and it sheds new light on the screening in dense electrolytes and the fitting of structural forces [19]. Our results are important for the interpretation of measurements and effective interactions [19,45–47], because they show that species correlation functions can be superpositions of charge contributions and density contributions of the same order of magnitude. A fit using the asymptotic form (12) cannot be expected to be accurate on intermediate length scales. Furthermore, the transition from monotonic to oscillatory decay underpins wetting phenomena [48,49]. The existence of multiple coexisting species-dependent decay lengths implies that addressable wetting could be achieved. Tuning the asymptotic correlations may also be used to control colloidal dispersions, for instance, to prevent aggregation [6] and to switch effective potentials by tuning the salt concentration [50]. It might be promising to construct complex interactions to achieve a rich crossover structure, for instance, in complex plasmas [51], colloid-polymer mixtures [52], and colloidal fluids [53].

The authors would like to thank M. Oettel, R. Kjellander, and R. Evans for insightful discussions. A. A. L. acknowledges the support of the Winton Programme for the Physics of Sustainability.

*andreas.haertel@physik.uni-freiburg.de

[1] D. F. Evans and H. Wennerström, *The Colloidal Domain* (Wiley-Blackwell, New York, 1999).
[2] M. V. Fedorov and A. A. Kornyshev, Chem. Rev. **114**, 2978 (2014).
[3] D. J. Bozym, B. Uralcan, D. T. Limmer, M. A. Pope, N. J. Szamreta, P. G. Debenedetti, and I. A. Aksay, J. Phys. Chem. Lett. **6**, 2644 (2015).
[4] D. T. Limmer, Phys. Rev. Lett. **115**, 256102 (2015).
[5] B. Uralcan, I. A. Aksay, P. G. Debenedetti, and D. T. Limmer, J. Phys. Chem. Lett. **7**, 2333 (2016).
[6] H. Zhang, K. Dasbiswas, N. B. Ludwig, G. Han, B. Lee, S. Vaikuntanathan, and D. V. Talapin, Nature (London) **542**, 328 (2017).
[7] P. Attard, Electrolytes and the electric double layer, in *Advances in Chemical Physics* (John Wiley & sons, inc, New York, 2007), Vol. 92, pp. 1–159.
[8] Y. Levin, Rep. Prog. Phys. **65**, 1577 (2002).
[9] R. Evans, R. J. F. Leote de Carvalho, J. R. Henderson, and D. C. Hoyle, J. Chem. Phys. **100**, 591 (1994).
[10] P. Attard, Phys. Rev. E **48**, 3604 (1993).
[11] R. J. F. Leote de Carvalho and R. Evans, Mol. Phys. **83**, 619 (1994).
[12] Y. Zeng and R. von Klitzing, Langmuir **28**, 6313 (2012).
[13] M. A. Gebbie, H. A. Dobbs, M. Valtiner, and J. N. Israelachvili, Proc. Natl. Acad. Sci. USA **112**, 7432 (2015).
[14] A. M. Smith, A. A. Lee, and S. Perkin, Phys. Rev. Lett. **118**, 096002 (2017).
[15] A. B. McEwen, H. L. Ngo, K. LeCompte, and J. L. Goldman, J. Electrochem. Soc. **146**, 1687 (1999).
[16] Y. Zhu, S. Murali, M. D. Stoller, K. J. Ganesh, W. Cai, P. J. Ferreira, A. Pirkle, R. M. Wallace, K. A. Cychosz, M. Thommes, D. Su, E. A. Stach, and R. S. Ruoff, Science **332**, 1537 (2011).

[17] X. Yang, C. Cheng, Y. Wang, L. Qiu, and D. Li, Science **341**, 534 (2013).
[18] M. Moazzami-Gudarzi, T. Kremer, V. Valmacco, P. Maroni, M. Borkovec, and G. Trefalt, Phys. Rev. Lett. **117**, 088001 (2016).
[19] S. Schön and R. von Klitzing, Beilstein J. Nanotechnol. **9**, 1095 (2018).
[20] C. Grodon, M. Dijkstra, R. Evans, and R. Roth, J. Chem. Phys. **121**, 7869 (2004).
[21] J. Baumgartl, R. P. A. Dullens, M. Dijkstra, R. Roth, and C. Bechinger, Phys. Rev. Lett. **98**, 198303 (2007).
[22] A. Statt, R. Pinchaipat, F. Turci, R. Evans, and C. P. Royall, J. Chem. Phys. **144**, 144506 (2016).
[23] M. J. Grimson and G. Rickayzen, Chem. Phys. Lett. **86**, 71 (1982).
[24] Z. Tang, L. E. Scriven, and H. T. Davis, J. Chem. Phys. **97**, 494 (1992).
[25] D. Boda and D. Henderson, J. Chem. Phys. **112**, 8934 (2000).
[26] B. Rotenberg, O. Bernard, and J.-P. Hansen, J. Phys. Condens. Matter **30**, 054005 (2018).
[27] H. J. Limbach, A. Arnold, B. A. Mann, and C. Holm, Comput. Phys. Commun. **174**, 704 (2006).
[28] A. Arnold, O. Lenz, S. Kesselheim, R. Weeber, F. Fahrenberger, D. Roehm, P. Košovan, and C. Holm, in *Meshfree Methods for Partial Differential Equations VI*, Lecture Notes in Computational Science and Engineering, edited by M. Griebel and M. A. Schweitzer (Springer, New York, 2013), Vol. 89, pp. 1–23.
[29] J.-P. Hansen and I. R. McDonald, *Theory of Simple Liquids*, 4th ed. (Elsevier, New York, 2013).
[30] R. Kjellander and D. Mitchell, Chem. Phys. Lett. **200**, 76 (1992).
[31] M. E. Fisher and B. Wiodm, J. Chem. Phys. **50**, 3756 (1969).
[32] J. R. Henderson and Z. A. Sabeur, J. Chem. Phys. **97**, 6750 (1992).
[33] H. Hansen-Goos and R. Roth, J. Phys. Condens. Matter **18**, 8413 (2006).
[34] J. G. Kirkwood, J. Chem. Phys. **7**, 919 (1939).
[35] See Supplemental Material at http://link.aps.org/supplemental/10.1103/PhysRevLett.121.075501 for a PDF document containing simulation results for asymmetric ions and a comparison between theory and experimental data. The document includes Refs. [14,36–40].
[36] A. M. Smith, A. A. Lee, and S. Perkin, J. Phys. Chem. Lett. **7**, 2157 (2016).
[37] S. W. Coles, A. M. Smith, M. V. Fedorov, F. Hausen, and S. Perkin, Faraday Discuss. **206**, 427 (2018).
[38] C. S. Santos, N. S. Murthy, G. A. Baker, and E. W. Castner, J. Chem. Phys. **134**, 121101 (2011).
[39] J.-C. Soetens, C. Millot, B. Maigret, and I. Bakó, J. Mol. Liq. **92**, 201 (2001).
[40] M. Oettel, S. Görig, A. Härtel, H. Löwen, M. Radu, and T. Schilling, Phys. Rev. E **82**, 051404 (2010).
[41] M. Parrinello and M. P. Tosi, Riv. Nuovo Cim. **2**, 1 (1979).
[42] G. Stell, K. C. Wu, and B. Larsen, Phys. Rev. Lett. **37**, 1369 (1976).
[43] A. A. Lee, C. S. Perez-Martinez, A. M. Smith, and S. Perkin, Phys. Rev. Lett. **119**, 026002 (2017).
[44] R. Evans, J. R. Henderson, D. C. Hoyle, A. O. Parry, and Z. A. Sabeur, Mol. Phys. **80**, 755 (1993).
[45] D. Gottwald, C. N. Likos, G. Kahl, and H. Löwen, Phys. Rev. Lett. **92**, 068301 (2004).
[46] D. Léger and D. Levesque, J. Chem. Phys. **123**, 124910 (2005).
[47] A. R. Denton, Phys. Rev. E **96**, 062610 (2017).
[48] A. A. Chernov and L. V. Mikheev, Phys. Rev. Lett. **60**, 2488 (1988).
[49] J. R. Henderson, Phys. Rev. E **50**, 4836 (1994).
[50] Y. Li, M. Girard, M. Shen, J. A. Millan, and M. O. de la Cruz, Proc. Natl. Acad. Sci. USA **114**, 11838 (2017).
[51] G. E. Morfill and A. V. Ivlev, Rev. Mod. Phys. **81**, 1353 (2009).
[52] J. M. Brader, M. Dijkstra, and R. Evans, Phys. Rev. E **63**, 041405 (2001).
[53] A. J. Archer, D. Pini, R. Evans, and L. Reatto, J. Chem. Phys. **126**, 014104 (2007).